Biogeosciences Discuss., 10, 8685–8713, 2013
www.biogeosciences-discuss.net/10/8685/2013/
doi:10.5194/bgd-10-8685-2013

Biogeosciences Discussions
Open Access

Nitrification and its oxygen consumption along the turbid Changjiang River plume

S. S.-Y. Hsiao[1], T.-C. Hsu[1], J.-W. Liu[2], X. Xie[2], Y. Zhang[2], J. Lin[2], H. Wang[2], J.-Y. T. Yang[2], S.-C. Hsu[1], M. Dai[2], and S.-J. Kao[1,2]

[1]Earth System Science Program, Taiwan International Graduate Program, Research Center for Environmental Changes, Academia Sinica, Taipei, Taiwan
[2]State Key Laboratory of Marine Environmental Science, Xiamen University, Xiamen, China

Received: 30 March 2013 – Accepted: 24 April 2013 – Published: 24 May 2013

Correspondence to: S.-J. Kao (sjkao@gate.sinica.edu.tw)

Published by Copernicus Publications on behalf of the European Geosciences Union.

Abstract

Nitrification rates of bulk water (NR_b) and particle free (NR_{pf}, particle > 3 µm eliminated) were determined along the Changjiang River plume in August 2011 by nitrogen isotope tracer technique. Dissolved oxygen (DO), community respiration rate (CR), nutrients, dissolved organic nitrogen, total suspended matter (TSM), particulate organic carbon/nitrogen (POC/PON), acid-leachable iron and manganese on suspended particles and both archaeal and *β*-proteobacterial *amo*A abundance on size-fractioned particle (> 3 µm and 0.22–3 µm) were measured. The NR_b ranged from undetectable up to 4.6 µmol L^{-1} d^{-1} peaking at salinity of ~ 29. NR_b values were positively correlated with ammonia concentration suggesting the importance of substrate in nitrification. In river mouth and inner plume, NR_b was much higher than NR_{pf} indicating nitrifying bacteria is mainly particle-associated, which was supported by *amo*A gene abundance and regression analysis of TSM and NR_b. The estimated oxygen demand of nitrification accounted for 0.4 % to 317 % of CR. The nitrification oxygen demand is much higher than Redfield model's estimation (23 %) indicating that oxygen might not be the sole oxidant though DO was sufficient (> 58 µmol kg^{-1}). The excess nitrification oxygen demand showed tendency to occur at lower DO samples accompanying with higher acid-leachable Fe/Mn, which implied reactive Fe^{3+}/Mn^{4+} may play a role as oxidant in nitrification process. Stoichiometric calculation suggested reactive Fe on particles was even 10-fold the oxidant demand for complete ammonia oxidation along all areas of the plume. The involvement of reactive iron and manganese in nitrification process in oxygenated water further complicated the nitrogen cycling in turbid river plume.

1 Introduction

Estuaries and coastal seas receiving natural and anthropogenic materials from rivers serve as an important reactor for chemical/physical transformation. Growing population and human activities in past few decades had enhanced riverine nutrient loads

BGD
10, 8685–8713, 2013

more than 5-fold, which profoundly impacted the aquatic environment of land–ocean boundary (Dai et al., 2011; Howarth and Marino, 2006). Nitrogen is one of the most influential elements among the enhanced nutrients (Galloway et al., 2004; Gunnarsson et al., 2000; Howarth and Marino, 2006) that may lead to eutrophication, subsequently promote the oxygen consumption resulting in more severely hypoxia or "dead zone" which disrupts estuarine and coastal ecosystem (Rabalais et al., 2002; Smith et al., 2006; Galloway et al., 2004; Ravishankara et al., 2009). The original nitrogen cycle is thus altered.

One of the most affected processes is nitrification, in which ammonium is oxidized to nitrate and nitrous oxide, a greenhouse gas, is produced as a byproduct. Anthropogenic-enhanced nitrification becomes an important oxygen consuming process contributing to the establishment of hypoxia. In British Columbia fjord (Grundle and Juniper, 2011), Delaware River (Lipschultz et al., 1986), Pearl River (Dai et al., 2008), Narragansett Bay (Berounsky and Nixon, 1993) and Scheldt estuary (Gazeau et al., 2005), nitrification can contribute 20–30 % of total oxygen consumption, and even up to 64 % in Mississippi River estuary (Pakulski et al., 1995). Besides, the exacerbated nitrification may also contribute to alkalinity consumption that subsequently enhances ocean acidification (Hu and Cai, 2011). In spite of the highlighted importance, the knowledge about nitrification in land–ocean boundary remains incomplete.

Recent culture-based and field experiments in freshwater and marine upwelling systems revealed that nitrifiers tend to attach particles where ammonia adsorption may occur to stimulate nitrification (Xia et al., 2009; Wang et al., 2010; Fussel et al., 2012). One distinctive feature for Asian rivers is that enhanced nutrient fluxes generally accompany with huge amount of suspended sediments which are sourced from soil erosion (Syvitski et al., 2005; Milliman and Syvitski, 1992) and result in highly turbid coastal and shelf water, for example, the East China Sea shelf as evidenced by satellite images (Fig. 1a). Previous field studies in the Seine River and Scheldt estuary observed a positive relation between TSM concentration and nitrification potential based on nutrient monitoring and model calculation (Brion et al., 2000; Andersson et al., 2006). To

BGD
10, 8685–8713, 2013

our knowledge there was only one single paper implemented direct measurements of nitrification rate on particulate fraction in estuary (Berounsky and Nixon, 1993); however, their results in Narragansett bay with low suspended particle concentration did not support the importance of particle on nitrification.

In this study, we selected the East China Sea shelf where remarkable amount of nutrients and sediments are received from the Changjiang (Yangtze) River, whose water and sediment discharge are the third and the fourth largest, respectively, in the world (Milliman and Syvitski, 1992; Syvitski et al., 2005). The annual suspended sediment discharge is ca. 400 $\mathrm{Mt\,yr^{-1}}$ (Chen et al., 2001) though decreasing after Three-Gorges Dam construction. Presently, the annual load of dissolved inorganic nitrogen (DIN) is $\sim 10.8 \times 10^{10}$ ($\mathrm{mol\,yr^{-1}}$), which is 8 times higher compared with that in 1960 (Wang, 2006; Chai et al., 2009). The summer hypoxia in the plume region was first reported in 1959, since then it expanded eastward with a rising nutrient load (Wang, 2009; Ning et al., 2011; Zhu et al., 2011; Wang et al., 2012). The intensified stratification due to fresh water input and high temperature in summer blocks oxygen supply through air-sea interface, meanwhile the intruding Taiwan warm current with oxygenated water from the south affects the lateral oxygen exchange; thus, shapes up the zonal pattern of the hypoxia off Changjiang River estuary (Wang, 2009).

In the Changjiang Plume, the interplay of nutrient and suspended sediment in nitrification rate has never been investigated before, particularly, during summer high flow with great potential of hypoxia. Our cruise was set during flood season to examine the potential role of particle in nitrification and oxygen consumption in the river plume. This is the first study to explore specifically particle-associated nitrification in turbid shelf water by using stable isotope tracer method. Positive yet distinctive relations between nitrification rate and TSM were observed in the inner shelf and river mouth. More surprisingly, at some stations ferric Fe might serve as electron acceptor in nitrification reaction besides oxygen. To our knowledge, this phenomenon had never been documented before in aerobic water column.

BGD
10, 8685–8713, 2013

2 Material and method

2.1 Sampling

Our cruise was conducted during 15–24 August 2011, one week after typhoon Muifa passed through the East China Sea (6–7 August, see trajectory in Fig. 1a). Apparently, Muifa disturbed the water column off the Changjiang River mouth.

Water samples were collected roughly along two offshore transects starting from the river mouths of Changjiang and Qiantang River toward the shelf (Fig. 1b). The sampling sites were classified into three zones including river mouth, inner plume and outer plume based on salinity difference and geographical feature (Fig. 1b). Those stations with salinity lower than 20 were classified as river mouth. The most offshore stations Y4 and Y5 were classified as outer plume where are influenced by warm and saline Taiwan warm current (Wang, 2009). The other stations within salinity of 20 to 28 were classified as inner plume. A turbidity front appeared at the salinity of ∼22 (see Tseng et al., 2013, for spatial distribution of TSM), and distinctive correlations between TSM and nitrification rate of those stations support our zonal classification (see below). Meanwhile, according to the temperature distribution (see Tseng et al., 2013), we know the upwelling had occurred and outcropped at the seaward side of the turbidity front. In fact, most of the inner plume stations were located in upwelling zone. We also repeated our sampling 3 times at Sta. Y3 (named as 1Y3, 2Y3 and 3Y3) in 15, 19 and 22 August, respectively.

Judged from the daily water discharge curve (Fig. 1c) we know the water discharge in 2011 is smaller when compared with that of long-term mean monthly water discharge. Also, in such a large watershed, typhoon seems to play insignificant role in water discharge, which declined gradually after the peak in late June although there was a small jump in discharge followed up the Muifa that might be induced by typhoon rain. Therefore our cruise was still representative of the summer high flow condition.

BGD
10, 8685–8713, 2013

2.2 Hydrographical and chemical data

Vertical profiles of salinity, temperature and dissolved oxygen were obtained by CTD profiling system (SBE 911, SeaBird Co.). The dissolved oxygen data were calibrated by discrete measurements using Winkler method.

Water sample were collected with 12 L Niskin bottles for determination of dissolved oxygen, nutrients, total suspended material (TSM), particulate organic carbon/nitrogen and acid-leachable metals.

Nutrient samples were all analyzed on-deck. Ammonium was analyzed by the indophenol blue spectrophotometric method (Pai et al., 2001). Nitrite and nitrate were measured by AA3 system (Dai et al., 2011). The detection limits for ammonium, nitrite and nitrate were 0.16, 0.02 and 0.07 $\mu mol\,L^{-1}$, respectively. TSM sample were collected by filtering 1–4 L of water sample onto pre-combusted Whatman GF/F membrane. This glass fiber membrane was further analyzed for POC/PON by elemental analyzer detailed in Kao et al. (2012). DON was analyzed by persulfate oxidation method (Bronk et al., 2000) with detection limit of 0.6 $\mu mol\,L^{-1}$. Reactive (acid-leachable) metal on TSM sample were collected by filtering 0.25–1 L of water onto 0.45 µm acid-washed polycarbonate membrane. The filters were extracted by using 1N hydrochloric acid for 16 h (Kao et al., 2004) in a test tube and then centrifuged; the acid extract was further analyzed by inductively coupled plasma mass spectrometry (ICP-MS) (Hsu et al., 2004). The detection limit for Mn, Fe and Al were 0.89, 139 and 60 $\mu g\,L^{-1}$, which are 2 orders of magnitude below the measured concentration.

2.3 Incubation experiments

Nitrification rate (NR) was measured by stable isotopic tracer method (Lipschultz et al., 1986). For bulk nitrification rate (NR_b), at each depth,six 250 mL narrow-necked gas tight glass bottles were overflowed for more than 2-fold volume and sealed without any headspace. Then $^{15}NH_4Cl$ was injected to a final concentration of 50 $nmol\,L^{-1}$ in each bottle for 3, 6 and 12 h dark incubation (duplicate) in a tank with continuous circulation

BGD
10, 8685–8713, 2013

of surface sea water. The control sample was directly filtered and stored frozen without incubation. The incubation was terminated and immediately followed by filtering through 0.22 µm polycarbonate membrane and stored frozen at −20 °C until laboratory analysis. The change of ^{15}N content in nitrate and nitrite pool was determined by denitrifier method (Casciotti et al., 2002; McIlvin and Casciotti, 2011; Sigman et al., 2001). The regression coefficient of the time course curves of ^{15}N content in nitrate and nitrite pool were better than 0.8. The incubation of particle-free nitrification rate (NR_{pf}) was implemented after removing particle by using 3 µm polycarbonate membrane (Berounsky and Nixon, 1993). NR_{pf} was conducted only for Stas. Y0, 2Y3 and Y5.

The natural nitrification rate was calculated by the following equation:

$$R_{NO_x} = \frac{d[^{15}N]}{dt} \times \frac{\left[^{14}NH_4^+\right] + \left[^{15}NH_4^+\right]}{\left[^{15}NH_4^+\right]}$$

where R_{NO_x} is the nitrification rate, t is the incubation time, $[^{15}N]$ is the concentration of ^{15}N in nitrate plus nitrite pool in sample, and $[^{14}NH_4^+]$ and $[^{15}NH_4^+]$ are the observed natural ammonium concentration and artificial addition of stable isotopic tracer ($^{15}NH_4^+$), respectively. We used NO_x since in our method both NO_3^- and NO_2^- were included.

The community respiration rate (CR) was determined by the decrement in dissolved oxygen content after 24 h of incubation in darkness. Sampled waters were aliquot into duplicate 100 mL DO bottles fully covered by aluminum foil and all bottled were submerged afterward in the tank with sea surface water circulation. The difference in O_2 concentration between the initial and the dark treatment was used to compute the CR.

2.4 Archaeal and β-proteobacterial functional gene abundance

Particulate-associated ammonia monooxygenase (*amo*A) gene abundance of Archaeal and β-proteobacterial along Changjiang plume was determined by quantitative polymerase chain reaction (qPCR) method described in (Hu et al., 2011). Particle

BGD
10, 8685–8713, 2013

samples were divided into size fractions of > 3 µm and 0.22–3 µm via a series filtering of 1–2 L water sample.

3 Results

Our sampling transect crossed salinity of 0.2 to 34.3 along Changjiang River plume (Fig. 2a). The dissolved oxygen over this transect ranged from 58 to 225 µmol L^{-1} (Fig. 2b). Only the bottom water of Sta. 2Y9a reached the threshold of hypoxia. The hypoxic area of this cruise (Liu et al., unpublished data of this cruise) was smaller compared with historical record (Wei et al., 2007; Zhu et al., 2011). This was likely due to the disturbance of typhoon Muifa. The salinity observed in the Qiantang River mouth was overall higher than that in the Changjiang River mouth which ranged from 9.3 to 17.7 (Fig. 3a) and dissolved oxygen content ranged from 157 to 189 µmol kg^{-1} (Fig. 3b).

Distribution of ammonium (Fig. 2c), nitrite (Fig. 2d), nitrate (Fig. 2e) and DON (Fig. 2f) along the plume transect showed distinctive patterns. The distributions of nitrate and DON resembled the salinity pattern. The highest concentration of nitrate (133 µmol L^{-1}) and DON (27 µmol L^{-1}) appeared at the Sta. Y0 accompanying with the lowest salinity. However, ammonium and nitrite exhibited the biological mediated pattern. The maximum ammonium (2.0 µmol L^{-1}) occurred at the 10 m depth at offshore sta.Y5 while the maximum of nitrite (1.0 µmol L^{-1}) appeared right below it at 20 m depth. A secondary maximum of ammonium (1.2 µmol L^{-1}) occurred at the bottom of near shore sta. Y2, which co-existed with the highest NR_b. In Qiantang River mouth, ammonium and nitrite were less than 1.0 and 0.2 µmol L^{-1}, respectively (Fig. 3c and d). Nitrate was ranged between 86.7–149 µmol L^{-1} (Fig. 3e) while DON ranged from 7.35 to 17.8 µmol L^{-1} (not shown because of limited measurements) Both nitrate (Fig. 3e) and DON were high in the freshwater end similar to that of the Changjiang transect.

TSM ranged over 2 orders of magnitude from 2.61–244 mg L^{-1} along Changjiang plume (Fig. 2h). TSM in the Qiantang River mouth (Fig. 3h) ranged between

BGD
10, 8685–8713, 2013

1150–3000 mg L^{-1} which is 1 order higher than the Changjiang River mouth due to intensive wave and tidal mixing. For other particulate-associated acid-leachable metals, such as Al, Fe and Mn, similar seaward descending patterns can be seen (Figs. 2i, 3i). These metals showed ~ 3 orders of magnitude variability in concentration. The percentage of acid-leachable metal on TSM ranged between 0.2–17.3 % for Al, 0.1–5.7 % for Fe and 0.03–2.5 % for Mn, respectively (data not shown). The concentrations of POC (not shown) and PON (Figs. 2j and 3f) were also in a wide range for more than 3 orders of magnitude. By contrast, the range of organic C/N ratio (4.7–6.6) was very narrow indicating the particulate organic matter was mainly marine sourced.

The NR_b along the plume was peaked at intermediate salinity and decreased seaward to undetectable at near surface water in the most offshore station. The maximum NR_b (4.6 µmol L^{-1} d^{-1}) occurred at near bottom of Sta. Y2 (S = 29) (Fig. 2g). The second maximum (2.0 µmol L^{-1} d^{-1}) occurred at Sta. N5 (S = 9.4) in the Qiantang River mouth (Fig. 3g). The NR_b in Qiantang River mouth ranged from 210 to 2000 nmol L^{-1} d^{-1} which was overall higher than Changjiang River mouth.

Significant positive linear correlations between NR_b and ammonium could be found (Fig. 4a) for inner plume and river mouth and the two correlations were almost identical. In fact, only the two surface water samples in outer plume, which contained the highest ammonium but lowest NR_b, deviated from the regression. As for TSM (Fig. 4b), the distinctive correlations between NR_b and TSM occurred in inner plume (Slope = 13.2, intercept = 134) and river mouth (Slope = 0.33, intercept = 92); yet, in outer plume TSM is too low revealing no correlation with NR_b. For river mouth and inner plume, all other particulate-associated parameters including POC/PON and reactive Al/Fe/Mn possessed similar pattern as TSM toward NR_b, and the statistic value of these linear regressions were listed in Table 2. The most significant linear correlation was found between NR_b and reactive Mn in inner plume.

For DON, except the river mouth with wider range of DON showing a negative correlation with NR_b, the narrow range of DON (5–8 µmol L^{-1}) for inner and outer plume (Fig. 4c) revealed no correlation with NR_b. The CR values ranged

BGD
10, 8685–8713, 2013

between 1.21–10.79 µmol O_2 L^{-1} d^{-1} along the Changjiang River transect. The CR in the Qiantang River mouth was not analyzed. Put all available data together, we found a positive linear correlation between ammonium and CR (Fig. 4d), which indicated that aerobic degradation of organic matter was the major source of ammonium which may fuel the nitrification.

The particulate-associated *amo*A gene abundance of archaeal and β-proteobacterial, NR_b and NR_{pf} were shown in Table 1. We can see both archaeal and β-proteobacterial *amo*A gene abundance were 1–2 orders of magnitude higher at river mouth and inner plume when comparing with that in outer plume and more than 98 % of β-proteobacterial *amo*A presents on larger particles (> 3 µm) when TSM concentrations were high. In the river mouth and inner plume, NR_{pf} occupied less fraction of NR_b indicating nitrification prefers to occur on particles. By contrast, in the outer plume more than 62 % of β-proteobacterial *amo*A and more than 83 % of archaeal *amo*A was found in the size fraction of 0.22–3 µm with NR_{pf} occupied a larger fraction of NR_b and at one single depth NR_{pf} even higher than NR_b. The higher fraction of NR_{pf} in bulk nitrification indicates the fraction of > 3 µm is less important in outer plume; noteworthy that during filtration we might eliminate larger phytoplankton (competitor) or grazers. The super saturated DO at the subsurface of Y5 station is supportive to the idea of competitor elimination.

4 Discussion

4.1 The interplay between nitrification and environmental parameters

In the perspective of substrates supply, the nitrification rate should be constrained by ammonium and oxygen availability. The observed positive correlation between NR_b and ammonium concentration (Fig. 4a) indicated that ammonium may play an important role in nitrification at the inner plume and the river mouth where oxygen was sufficient. In addition, the range of NR_b (0–4.6 µmol L^{-1} d^{-1}) along the Changjiang River plume

BGD
10, 8685–8713, 2013

was similar to that of Rhone River plume (0–4.2 $\mu mol\,L^{-1}\,d^{-1}$; Bianchi et al., 1999) and Tamar estuary (0–3 $\mu mol\,L^{-1}\,d^{-1}$; Owens, 1986); all of those areas have ammonium concentration less than 3 $\mu mol\,L^{-1}$. However, our NR_b is lower when comparing with the Mississippi River estuary (up to 13.4 $\mu mol\,L^{-1}\,d^{-1}$; Pakulski et al., 1995), Scheldt Estuary (up to 16.8 $\mu mol\,L^{-1}\,d^{-1}$; Somville, 1984; Andersson et al., 2006), Narragansett Bay (up to 11.0 $\mu mol\,L^{-1}\,d^{-1}$; Berounsky and Nixon, 1993) and Pearl River estuary (up to 12.5 $\mu mol\,L^{-1}\,d^{-1}$; Dai et al., 2008). The higher NR_b in those estuaries is likely caused by higher ammonium concentration (> 3 $\mu mol\,L^{-1}$) indicating the importance of ammonium supply. However, some unraveled factors might also play a role, such as that reported in the cold British fjord where ammonium concentration was higher (0–5 $\mu mol\,L^{-1}$) but NR_b was lower (0.32–0.48 $\mu mol\,L^{-1}\,d^{-1}$) (Grundle and Juniper, 2011).

On the other hand, in outer plume the highest ammonium with the lowest NR_b appeared in the subsurface at Y5 station. The unexpected low nitrification under high substrate availability was probably due to the photoinhibition (Mackey et al., 2011; Merbt et al., 2012) in the relative clear surface seawater.

Nitrite concentration was narrowly ranged between 0.1–0.6 $\mu mol\,L^{-1}$ except that at outer plume subsurface and none correlation between nitrite and NR_b along the Changjiang plume was observed. Since nitrite is the intermediate compound in nitrification process, such wider range of ammonium and NR_b with limited nitrite variability may imply nitrite oxidation was close-coupled to ammonia oxidation and left insignificant amount of nitrite along the Changjiang River plume. However, in the outer plume subsurface, we can see nitrite accumulated beneath the layer of ammonium maximum. Previous studies indicated the nitrite maximum may result from uncoupled oxidation of NH_4^+ and NO_2^- during nitrification which leads to NO_2^- buildup if the microbial populations responsible for each step are spatially segregated within the water column (Lomas and Lipschultz, 2006). In our case, the nitrification rate in the nitrite maximum layer was under detection limit indicating that nitrite was not sourced from ammonium oxidation. Alternatively, NO_2^- production may occur during incomplete NO_3^- assimilation by phytoplankton, particularly when light stressed (Lomas and Lipschultz, 2006). We

BGD
10, 8685–8713, 2013

do not have sufficient data to go deeper for nitrite accumulation. However, our data clearly presented that in the outer plume when TSM concentration was decreased the light intensity will turn into an important factor exerting the assimilation and nitrification to compete for NH_4^+ in water column and allowing phytoplankton and nitrifying microbes to contribute jointly to the vertical distribution of different nitrogen species. DON was thought to be an important substrate in the upper open ocean for remineralization (Knapp et al., 2011); however, except the negative relation between DON and NR_b in river mouth, no positive correlation between DON and NR_b was observed implying high turnover rate of labile DON or DON was not an important source supplying ammonium for nitrification in our study area. The negative correlation in river mouth may just illustrate a higher DON supply from the river end, but NR_b was not influenced.

Ammonium oxidation is carried out by ammonia oxidizing archaea (AOA) and ammonia oxidizing bacteria (AOB). The *amo*A gene abundance of archaeal and β-proteobacterial on both > 3 µm and 0.22–3 µm fractions indicated that archaeal ammonia oxidizers were dominant along the Changjiang River plume (Table. 1). Both archaeal and β-proteobacterial ammonia oxidizer preferred to inhabit on > 3 µm particulate fraction in turbid river mouth and inner plume. This result may imply the particulate organic matter to be the potential source of ammonia for nitrifier to form biofilm and develop their population (Belser, 1979). Oppositely, in outer plume contained much fewer TSM (2.4–10.5 $mg\,L^{-1}$) nitrifiers were found to be abundant in 0.22–3 µm fraction.

The positive correlation between TSM and nitrification had been addressed in previous researches (Xia et al., 2009; Wang et al., 2010). The *amo*A abundance and NR results also support that ammonia oxidizer was mainly particulate associated. However, distinctive correlations (Fig. 4b) observed in the same river plume were firstly reported. The slope of the linear regression for river mouth was only 1/5 that of the inner plume. Since the PON content (%) on TSM (can be derived from Fig. 2h and j) was significantly higher for the inner plume than the river mouth ($p = 0.0046$, unpaired t test), we suspected that enriched PON can provide more ammonia efficiently.

BGD
10, 8685–8713, 2013

4.2 Reactive Fe as oxidant supply for nitrification in turbid river plume

Our CR range (1.21–10.79 $\mu mol\,L^{-1}\,d^{-1}$) broadly agreed with that reported in the East China Sea affected by Changjiang dilute water though some stations may have CR up to 34.3 $\mu mol\,L^{-1}\,d^{-1}$ (Chen et al., 2009). We assume Muifa well mixed the water column of our studied area before our cruise and the stratification started to reform afterward. In our cruise period the low oxygen content (~ 50 % saturation) in water column below 20 m depth was thus resulted from oxygen consumption within 1–2 weeks or so; the oxygen consumption rate can be roughly estimated to be ~ 10 $\mu mol\,L^{-1}\,d^{-1}$. This number is consistent with our observations.

It is well-known that oxygen is consumed during nitrification following the organic decomposition. According to the Redfield model (Redfield et al., 1963), total 138 mol of oxygen (O_2) is required to complete the mineralization of one mole of organic matter (Eq. 1), among which 32 mol of oxygen is required to fully oxidize 16 mole of ammonia (1 mol NH_3 to 2 mol O_2 in Eq. 2) to nitrate.

$$(CH_2O)_{106}(NH_3)_{16}(H_3PO_4)_1 + 138\,O_2 \rightarrow 106\,CO_2 + 16\,NO_3^- + PO_4^{3-} + 122\,H_2O + 19\,H^+ \quad (1)$$

$$NH_3 + 2\,O_2 \rightarrow HNO_3 + H_2O \quad G^0 = -270.2\,kJ\,mol^{-1} \quad (2)$$

Therefore, the theoretical percentage of oxygen consumption via nitrification can be derived to be 23.2 %. This estimation was practical in some previous estuarine studies (Berounsky and Nixon, 1993; Cooper, 1984; Grundle and Juniper, 2011; Lipschultz et al., 1986). Based on the molar ratio in Eq. (2), we can back calculate the nitrification-associated oxygen demand (NOD) by using the bulk nitrification rate (NR_b) we measured in incubation experiment. By dividing the estimated NOD by CR we obtain the proportion of oxygen consumption via nitrification. Interestingly, the percentage of oxygen consumption by bulk nitrification ranged from 0.4–318 %, among which 13 data from inner plume exceeded the Redfield model estimation of 23.2 % (Fig. 5a). The excess oxygen consumption may result from allochthonous ammonia, which had been

BGD
10, 8685–8713, 2013

reported in other estuaries as well as surface sediments (Cooper, 1984; Dai et al., 2008; Pakulski et al., 1995; Seitzinger et al., 1984; Seitzinger, 1987).

Surprisingly, 5 data from the inner plume even surpass the measured total oxygen consumption. Since CR and NR_b were both for bulk water sample, such abnormally high oxygen demand may imply that oxygen was not the sole electron acceptor in nitrification reaction. To our knowledge, this phenomenon was only documented once in surface sediments in Nueces estuary (Yoon and Benner, 1992).

Previous study had indicated that iron oxide and manganese oxide may support nitrification as oxidant in anaerobic sediments or oxygen minimum zone (Clement et al., 2005; Hulth et al., 1999; Luther et al., 1997; Luther and Popp, 2002; Vandenabeele et al., 1995). The hypothesized reactions can be written as Eq. (3) (Clement et al., 2005) and Eq. (4) (Luther and Popp, 2002).

$$NH_4^+ + 6\,FeOOH + 10\,H^+ \rightarrow NO_2^- + 6\,Fe^{2+} + 10\,H_2O \quad G^0 = -28.9\,kJ\,mol^{-1} \tag{3}$$

$$NO_2^- + MnO_2 + 2\,H^+ \rightarrow NO_3^- + Mn^{2+} + H_2O \quad G^0 = -56.0\,kJ\,mol^{-1} \tag{4}$$

Though oxygen was more thermodynamically favorable oxidant and sufficient in water column, the microenvironment in/upon particles may be oxygen-limited caused by high microbial activity in this turbid and eutrophicated region.

The correlation between percentage of NOD in CR versus DO, community respiration rate and two alternative oxidants, reactive Fe and Mn, were shown in Fig. 5. In the entire study area, oxygen was sufficient along the plume that the lowest oxygen content was 58 $\mu mol\,L^{-1}$ or 25.8 % of saturation. Although no correlation can be seen between estimated NOD/CR (%) and DO, higher NOD/CR (%) showed a tendency to occur toward DO < 200 $\mu mol\,L^{-1}$. For DO > 200 $\mu mol\,L^{-1}$, the Redfield model works well. On the other hand, significant linear correlations were found between the NOD/CR (%) and reactive Fe/Mn on particles in inner plume (Fig. 5c and d) implying that reactive Fe/Mn of particle may participate in the nitrification process as oxidant.

Similar to the oxygen demand estimation presented above, stoichiometric calculation was performed to evaluate if the reactive Fe/Mn were sufficient to support the oxidant

BGD
10, 8685–8713, 2013

demand for nitrification. We used goethite (FeOOH) and manganese oxide (MnO_2), which are both common in natural aerobic environment, in our estimation. According to Eqs. (3) and (4), six mole of goethite was required for one mole of ammonia to oxidize to nitrite and one mole of manganese oxide was required for one mole of nitrite to oxidize to nitrate. Therefore, we can estimate Fe and Mn demand by using NR_b when assuming nitrification was entirely relied on Fe(III) and Mn(IV). In Table 3, we presented the observed reactive Fe/Mn in water column versus nitrification-associated Fe(III) and Mn(IV) demand. Obviously, observed reactive Fe is 10× higher than that to support measured nitrification. Yet, the reactive Mn was insufficient to support nitrite oxidation. Our estimation only presented the upper bound of Fe(III) and Mn(IV) demand, and we clearly know O_2 must play a role. Previous study indicated that Mn(IV) mediated ammonia oxidation was also thermodynamically favorable, but this reaction required 3-fold of Mn(IV) than the nitrite oxidation (Hulth et al., 1999). Further investigations on the speciation of Fe/Mn and the coupling process of oxygen, Fe/Mn reduction and nitrification are needed.

The enhanced nitrification in eutrophicated estuaries had been thought to consume alkalinity to make ocean acidification worse (Dai et al., 2008). Conversely, the Fe/Mn mediated nitrification process consumes protons that mitigate the releasing of CO_2 to atmosphere. Nevertheless, how various oxidants interplay with nitrification to contribute to ocean acidification remains unclear. Two important issues required more attention: (1) Fe/Mn oxide may not be overlooked in hypoxia development in such turbid river plume; (2) since the N_2O yield of ammonia oxidation might link to the different forms of oxidant, reactive Fe/Mn might regulate the N_2O emission in turbid coastal environments.

5 Conclusions and implications

Nitrification and its oxygen consumption were investigated along the turbid Changjiang River plume. Our study suggested that ammonium plays a role in nitrification. Moreover,

BGD
10, 8685–8713, 2013

the *amo*A gene abundance and NR_{pf} determination revealed that both archaeal and β-proteobacterial ammonia oxidizer preferred attaching to suspended particles (> 3 µm). Microenvironment formed on particle surface benefits nitrification activity in two ways. First, ammonia can be supplied via ambient water or from in situ decomposition. The latter process was implied by the different slopes of TSM against NR_b from in inner shelf and river mouth. Second, under oxygen-limiting condition, nitrification activity can be maintained efficiently by utilizing metallic oxidant which avoids the oxygen competition with heterotrophic bacteria. Stoichiometric calculation indicated that reactive Fe in plume water was sufficient as oxidant to support full ammonia oxidation rate in our incubation experiment. The role of nitrification in the overall water column oxygen consumption may not be simply utilizing only oxygen as oxidant it also consumes metallic oxidant suspension from river. In addition, high oxygen demand of autotrophic nitrifier also implied that considering fraction of CR attributes to nitrification. When applying CR to estimate reminieralization of organic matter including nitrification, underestimation may occur because nitrifier may consume non-oxygen oxidant especially in turbid coastal and shelf water.

Acknowledgements. We are grateful to Shuen-Hsin Lin and Yi-Tang Huang for helping the ICP-MS analysis of particulate metal content and Zhouling Zhang for assisting the on-deck nutrient measurement. This research was supported by the National Science Council, Taiwan and the National Natural Science Foundation of China (NSFC 41176059, 2009CB421200).

References

Andersson, M. G. I., Brion, N., and Middelburg, J. J.: Comparison of nitrifier activity versus growth in the Scheldt estuary – a turbid, tidal estuary in northern Europe, Aquat. Microb. Ecol., 42, 149–158, doi:10.3354/Ame042149, 2006.

Belser, L. W.: Population ecology of nitrifying bacteria, Annu. Rev. Microbiol., 33, 309–333, doi:10.1146/annurev.mi.33.100179.001521, 1979.

Berounsky, V. M. and Nixon, S. W.: Rates of nitrification along an estuarine gradient in Narragansett Bay, Estuaries, 16, 718–730, doi:10.2307/1352430, 1993.

BGD
10, 8685–8713, 2013

Bianchi, M., Feliatra, and Lefevre, D.: Regulation of nitrification in the land–ocean contact area of the Rhone River plume (NW Mediterranean), Aquat. Microb. Ecol., 18, 301–312, doi:10.3354/Ame018301, 1999.

Brion, N., Billen, G., Guezennec, L., and Ficht, A.: Distribution of nitrifying activity in the Seine River (France) from Paris to the estuary, Estuaries, 23, 669–682, doi:10.2307/1352893, 2000.

Bronk, D. A., Lomas, M. W., Glibert, P. M., Schukert, K. J., and Sanderson, M. P.: Total dissolved nitrogen analysis: comparisons between the persulfate, UV and high temperature oxidation methods, Mar. Chem., 69, 163–178, doi:10.1016/S0304-4203(99)00103-6, 2000.

Casciotti, K. L., Sigman, D. M., Hastings, M. G., Bohlke, J. K., and Hilkert, A.: Measurement of the oxygen isotopic composition of nitrate in seawater and freshwater using the denitrifier method, Anal. Chem., 74, 4905–4912, doi:10.1021/Ac020113w, 2002.

Chai, C., Yu, Z., Shen, Z., Song, X., Cao, X., and Yao, Y.: Nutrient characteristics in the Yangtze River Estuary and the adjacent East China Sea before and after impoundment of the Three Gorges Dam, Sci. Total. Environ., 407, 4687–4695, 2009.

Chen, C. C., Shiah, F. K., Chiang, K. P., Gong, G. C., and Kemp, W. M.: Effects of the Changjiang (Yangtze) River discharge on planktonic community respiration in the East China Sea, J. Geophys. Res.-Oceans, 114, C03005, doi:10.1029/2008JC004891, 2009.

Chen, Z., Li, J., Shen, H., and Wang, Z.: Changjiang of China: historical analysis of discharge variability and sediment flux, Geomorphology, 41, 77–91, 2001.

Clement, J. C., Shrestha, J., Ehrenfeld, J. G., and Jaffe, P. R.: Ammonium oxidation coupled to dissimilatory reduction of iron under anaerobic conditions in wetland soils, Soil. Biol. Biochem., 37, 2323–2328, doi:10.1016/j.soilbio.2005.03.027, 2005.

Cooper, A. B.: Activities of benthic nitrifiers in streams and their role in oxygen-consumption, Microb. Ecol., 10, 317–334, doi:10.1007/Bf02015557, 1984.

Cooper, P. F., McBarnet, W., O'Donnell, D., McMahon, A., Houston, L., and Brian, M.: The treatment of run-off from a fertiliser plant for nitrification, denitrification and phosphorus removal by use of constructed wetlands: a demonstration study, Water Sci. Technol., 61, 355–363, doi:10.2166/Wst.2010.801, 2010.

Dai, M., Wang, L., Guo, X., Zhai, W., Li, Q., He, B., and Kao, S.-J.: Nitrification and inorganic nitrogen distribution in a large perturbed river/estuarine system: the Pearl River Estuary, China, Biogeosciences, 5, 1227–1244, doi:10.5194/bg-5-1227-2008, 2008.

BGD
10, 8685–8713, 2013

Dai, Z. J., Du, J. Z., Zhang, X. L., Su, N., and Li, J. F.: Variation of riverine material loads and environmental consequences on the Changjiang (Yangtze) Estuary in recent decades (1955–2008), Environ. Sci. Technol., 45, 223–227, 2011.

Fussel, J., Lam, P., Lavik, G., Jensen, M. M., Holtappels, M., Gunter, M., and Kuypers, M. M.: Nitrite oxidation in the Namibian oxygen minimum zone, Isme J., 6, 1200–1209, doi:10.1038/ismej.2011.178, 2012.

Galloway, J. N., Dentener, F. J., Capone, D. G., Boyer, E. W., Howarth, R. W., Seitzinger, S. P., Asner, G. P., Cleveland, C. C., Green, P. A., Holland, E. A., Karl, D. M., Michaels, A. F., Porter, J. H., Townsend, A. R., and Vorosmarty, C. J.: Nitrogen cycles: past, present, and future, Biogeochemistry, 70, 153–226, doi:10.1007/s10533-004-0370-0, 2004.

Gazeau, F., Gattuso, J. P., Middelburg, J. J., Brion, N., Schiettecatte, L. S., Frankignoulle, M., and Borges, A. V.: Planktonic and whole system metabolism in a nutrient-rich estuary (the Scheldt estuary), Estuaries, 28, 868–883, doi:10.1007/Bf02696016, 2005.

Grundle, D. S. and Juniper, S. K.: Nitrification from the lower euphotic zone to the sub-oxic waters of a highly productive British Columbia fjord, Mar. Chem., 126, 173–181, doi:10.1016/j.marchem.2011.06.001, 2011.

Gunnarsson, J., Bjork, M., Gilek, M., Granberg, M., and Rosenberg, R.: Effects of eutrophication on contaminant cycling in marine benthic systems, Ambio, 29, 252–259, doi:10.1579/0044-7447-29.4.252, 2000.

Howarth, R. W. and Marino, R.: Nitrogen as the limiting nutrient for eutrophication in coastal marine ecosystems: evolving views over three decades, Limnol. Oceanogr., 51, 364–376, 2006.

Hsu, S. C., Liu, S. C., Lin, C. Y., Hsu, R. T., Huang, Y. T., and Chen, Y. W.: Metal compositions of PM_{10} and $PM_{2.5}$ aerosols in Taipei during spring, 2002, Terr. Atmos. Ocean Sci., 15, 925–948, 2004, http://www.ocean-sci.net/15/925/2004/.

Hu, A. Y., Jiao, N. Z., and Zhang, C. L. L.: Community structure and function of planktonic crenarchaeota: changes with depth in the South China Sea, Microb. Ecol., 62, 549–563, doi:10.1007/s00248-011-9866-z, 2011.

Hu, X. P. and Cai, W. J.: An assessment of ocean margin anaerobic processes on oceanic alkalinity budget, Global Biogeochem. Cy., 25, GB3003, doi:10.1029/2010gb003859, 2011.

BGD
10, 8685–8713, 2013

Hulth, S., Aller, R. C., and Gilbert, F.: Coupled anoxic nitrification manganese reduction in marine sediments, Geochim. Cosmochim. Ac., 63, 49–66, doi:10.1016/S0016-7037(98)00285-3, 1999.

Kao, S. J., Horng, C. S., Roberts, A. P., and Liu, K. K.: Carbon-sulfur-iron relationships in sedimentary rocks from southwestern Taiwan: influence of geochemical environment on greigite and pyrrhotite formation, Chem. Geol., 203, 153–168, doi:10.1016/j.chemgeo.2003.09.007, 2004.

Kao, S. J., Yang, J. Y. T., Liu, K. K., Dai, M. H., Chou, W. C., Lin, H. L., and Ren, H. J.: Isotope constraints on particulate nitrogen source and dynamics in the upper water column of the oligotrophic South China Sea, Global Biogeochem. Cy., 26, GB2033, doi:10.1029/2011gb004091, 2012.

Knapp, A. N., Sigman, D. M., Lipschultz, F., Kustka, A. B., and Capone, D. G.: Interbasin isotopic correspondence between upper-ocean bulk DON and subsurface nitrate and its implications for marine nitrogencycling, Global Biogeochem. Cy., 25, GB4004, doi:10.1029/2010GB003878, 2011.

Lomas, M. W. and Lipschultz, F.: Forming the primary nitrite maximum: nitrifiers or phytoplankton?, Limnol. Oceanogr., 51, 2453–2467, 2006.

Lipschultz, F., Wofsy, S. C., and Fox, L. E.: Nitrogen-metabolism of the eutrophic Delaware River ecosystem, Limnol. Oceanogr., 31, 701–716, 1986.

Luther, G. W. and Popp, J. I.: Kinetics of the abiotic reduction of polymeric manganese dioxide by nitrite: an anaerobic nitrification reaction, Aquat. Geochem., 8, 15–36, 2002.

Luther, G. W., Sundby, B., Lewis, B. L., Brendel, P. J., and Silverberg, N.: Interactions of manganese with the nitrogen cycle: alternative pathways to dinitrogen, Geochim. Cosmochim. Ac., 61, 4043–4052, doi:10.1016/S0016-7037(97)00239-1, 1997.

Mackey, K. R. M., Bristow, L., Parks, D. R., Altabet, M. A., Post, A. F., and Paytan, A.: The influence of light on nitrogen cycling and the primary nitrite maximum in a seasonally stratified sea, Prog. Oceanogr., 91, 545–560, doi:10.1016/j.pocean.2011.09.001, 2011.

McIlvin, M. R. and Casciotti, K. L.: Technical updates to the bacterial method for nitrate isotopic analyses, Anal. Chem., 83, 1850–1856, doi:10.1021/ac1028984, 2011.

Merbt, S. N., Stahl, D. A., Casamayor, E. O., Marti, E., Nicol, G. W., and Prosser, J. I.: Differential photoinhibition of bacterial and archaeal ammonia oxidation, Fems Microbiol. Lett., 327, 41–46, doi:10.1111/j.1574-6968.2011.02457.x, 2012.

BGD
10, 8685–8713, 2013

Milliman, J. D. and Syvitski, J. P. M.: Geomorphic tectonic control of sediment discharge to the ocean – the importance of small mountainous rivers, J. Geol., 100, 525–544, 1992.
Ning, X., Lin, C., Su, J., Liu, C., Hao, Q., and Le, F.: Long-term changes of dissolved oxygen, hypoxia, and the responses of the ecosystems in the East China Sea from 1975 to 1995, J. Oceanogr., 67, 59–75, doi:10.1007/s10872-011-0006-7, 2011.
Owens, N. J. P.: Estuarine nitrification – a naturally-occurring fluidized-bed reaction, Estuar. Coast Shelf. S., 22, 31–44, doi:10.1016/0272-7714(86)90022-3, 1986.
Pai, S. C., Tsau, Y. J., and Yang, T. I.: pH and buffering capacity problems involved in the determination of ammonia in saline water using the indophenol blue spectrophotometric method, Anal. Chim. Acta, 434, 209–216, doi:10.1016/S0003-2670(01)00851-0, 2001.
Pakulski, J. D., Benner, R., Amon, R., Eadie, B., and Whitledge, T.: Community metabolism and nutrient cycling in the Mississippi River plume – evidence for intense nitrification at intermediate salinities, Mar. Ecol.-Prog. Ser., 117, 207–218, doi:10.3354/Meps117207, 1995.
Rabalais, N. N., Turner, R. E., and Wiseman, W. J.: Gulf of Mexico hypoxia, aka "The dead zone", Annu. Rev. Ecol. Syst., 33, 235–263, doi:10.1146/annurev.ecolsys.33.010802.150513, 2002.
Ravishankara, A. R., Daniel, J. S., and Portmann, R. W.: Nitrous oxide (N_2O): the dominant ozone-depleting substance emitted in the 21st Century, Science, 326, 123–125, doi:10.1126/science.1176985, 2009.
Redfield, A. C., Ketchum, B. H., and Richards, F. A.: The influence of organism on the composition of sea water, in: The Sea, edited by: Hill, M. N., Wiley-Interscience, New York, 26–77, 1963.
Seitzinger, S. P.: Nitrogen biogeochemistry in an unpolluted estuary – the importance of benthic denitrification, Mar. Ecol.-Prog. Ser., 41, 177–186, doi:10.3354/Meps041177, 1987.
Seitzinger, S. P., Nixon, S. W., and Pilson, M. E. Q.: Denitrification and nitrous-oxide production in a coastal marine ecosystem, Limnol. Oceanogr., 29, 73–83, 1984.
Sigman, D. M., Casciotti, K. L., Andreani, M., Barford, C., Galanter, M., and Bohlke, J. K.: A bacterial method for the nitrogen isotopic analysis of nitrate in seawater and freshwater, Anal. Chem., 73, 4145–4153, 2001.
Smith, V. H., Joye, S. B., and Howarth, R. W.: Eutrophication of freshwater and marine ecosystems, Limnol. Oceanogr., 51, 351–355, 2006.
Somville, M.: Use of nitrifying activity measurements for describing the effect of salinity on nitrification in the Scheldt Estuary, Appl. Environ. Microb., 47, 424–426, 1984.

BGD
10, 8685–8713, 2013

Syvitski, J. P. M., Vorosmarty, C. J., Kettner, A. J., and Green, P.: Impact of humans on the flux of terrestrial sediment to the global coastal ocean, Science, 308, 376–380, doi:10.1126/science.1109454, 2005.
Tseng, Y. F., Lin, J., Dai, M., and Kao, S. J.: Joint effect of freshwater plume and coastal upwelling on phytoplankton growth off the Changjiang River, Biogeosciences, this issue, 2013.
Vandenabeele, J., Vandewoestyne, M., Houwen, F., Germonpre, R., Vandesande, D., and Verstraete, W.: Role of autotrophic nitrifiers in biological manganese removal from groundwater containing manganese and ammonium, Microb. Ecol., 29, 83–98, 1995.
Wang, B.: Cultural eutrophication in the Changjiang (Yangtze River) plume: history and perspective, Estuar. Coast. Shelf S., 69, 471–477, 2006.
Wang, B.: Hydromorphological mechanisms leading to hypoxia off the Changjiang estuary, Mar. Environ. Res., 67, 53–58, 2009.
Wang, B., Wei, Q., Chen, J., and Xie, L.: Annual cycle of hypoxia off the Changjiang (Yangtze River) Estuary, Mar. Environ. Res., 77, 1–5, doi:10.1016/j.marenvres.2011.12.007, 2012.
Wang, H. Y., Shen, Z. Y., Guo, X. J., Niu, J. F., and Kang, B.: Ammonia adsorption and nitritation in sediments derived from the Three Gorges Reservoir, China, Environ. Earth Sci., 60, 1653–1660, doi:10.1007/s12665-009-0299-7, 2010.
Ward, B.: Nitrification in marine systems, in: Nitrogen in the Marine Environment, 2nd edn., edited by: Capone, D., Bronk, D., Mulholland, M., and Carpenter, E., Elsevier, Amsterdam, 199–261, 2008.
Wei, H., He, Y. C., Li, Q. J., Liu, Z. Y., and Wang, H. T.: Summer hypoxia adjacent to the Changjiang Estuary, J. Mar. Syst., 67, 292–303, doi:10.1016/j.jmarsys.2006.04.014, 2007.
Xia, X. H., Yang, Z. F., and Zhang, X. Q.: Effect of suspended-sediment concentration on nitrification in river water: importance of suspended sediment–water interface, Environ. Sci. Technol., 43, 3681–3687, doi:10.1021/Es8036675, 2009.
Yoon, W. B. and Benner, R.: Denitrification and oxygen-consumption in sediments of 2 south Texas estuaries, Mar. Ecol.-Prog. Ser., 90, 157–167, doi:10.3354/Meps090157, 1992.
Zhu, Z. Y., Zhang, J., Wu, Y., Zhang, Y. Y., Lin, J., and Liu, S. M.: Hypoxia off the Changjiang (Yangtze River) Estuary: oxygen depletion and organic matter decomposition, Mar. Chem., 125, 108–116, doi:10.1016/j.marchem.2011.03.005, 2011.

BGD
10, 8685–8713, 2013

Table 1. The particulate associated archaeal and β-proteobacterial *amo*A copies and the nitrification rate in bulk versus filtered water for three stations along the Changjiang River plume.

Class	Sta.	Depth	TSM	Nitrification rate		β-proteobacterial *amo*A		Archaeal *amo*A	
				Bulk	Filtered[a]	Parti.(> 3 μm)[b]	Parti.(0.22–3 μm)[b]	Parti.(> 3 μm)[b]	Parti.(0.22–3 μm)[b]
		(m)	($mg\,L^{-1}$)	($nmol\,L^{-1}\,d^{-1}$)	($nmol\,L^{-1}\,d^{-1}$)	($log_{10}(copy\,L^{-1})$)	($log_{10}(copy\,L^{-1})$)	($log_{10}(copy\,L^{-1})$)	($log_{10}(copy\,L^{-1})$)
River mouth	Y0	7	261.0	168.23 ± 0.02	18.87 ± 0.04	6.2 ± 5.6 (99 %)	4.1 ± 3.0 (1 %)	7.4 ± 6.8 (66 %)	7.1 ± 5.2 (34 %)
		3	170.2	49.97 ± 0.02	9.29 ± 0.01	5.3 ± 4.9 (98 %)	3.7 ± 2.8 (1 %)	7.2 ± 6.4 (100 %)	5.8 ± 4.4 (0 %)
Inner plume	2Y3	20	48.1	973.25 ± 0.73	71.15 ± 0.05	5.7 ± 4.5 (100 %)	3.3 ± 2.9 (0 %)	8.2 ± 6.5 (100 %)	5.0 ± 4.4 (0 %)
		10	22.1	408.28 ± 0.37	215.09 ± 0.02	–	–	–	–
		3	9.2	283.50 ± 0.11	152.97 ± 0.02	–	–	–	–
Outer plume	Y5	46	4.5	16.75 ± 0.01	73.60 ± 0.01	4.0 ± 3.3 (38 %)	4.2 ± 2.9 (62 %)	6.4 ± 5.4 (2 %)	8.2 ± 6.4 (98 %)
		3	10.5	BDL	BDL	BDL	2.8 ± 0.9	4.1 ± 3.4 (17 %)	4.9 ± 3.5 (83 %)

Nitrification rate was presented as mean ± standard deviation. BDL: below detection limit.
[a] Filtered: particles larger than 3 μm were removed in the incubation for nitrification rate measurement.
[b] Parti. stands for particulate sample and its size range. The percentage value in the parentheses indicates the relative contribution to total *amo*A abundance.

BGD
10, 8685–8713, 2013

Table 2. The statistical value between NR_b and particulate associated geochemical parameters.

Location		TSM	Reactive Fe	Reactive Mn	Reactive Al	POC	PON
River mouth	R^2	0.71	0.80	0.71	0.80	0.71	0.73
(n = 10)	p	0.05	0.02	0.05	0.02	0.05	0.04
Inner plume	R^2	0.56	0.54	0.54	0.30	0.33	0.42
(n = 26)	p	0.00	0.00	0.00	0.04	0.04	0.04

BGD
10, 8685–8713, 2013

Table 3. Estimated Fe(III) and Mn(IV) demand for nitrification and the observed concentrations.

Class	Sta.	Salinity	Depth (m)	Fe(III) demand[a] ($nmol\,L^{-1}\,d^{-1}$)	Reactive Fe ($nmol\,L^{-1}$)	Mn(IV) demand[b] ($nmol\,L^{-1}\,d^{-1}$)	Reactive Mn ($nmol\,L^{-1}$)
	N5	9.37	7	1.17×10^{4}	9.30×10^{5}	1.96×10^{3}	7.32×10^{2}
	N5	9.31	3	3.28×10^{3}	4.98×10^{5}	5.47×10^{2}	4.14×10^{2}
	N3	12.02	8	1.24×10^{3}	2.39×10^{5}	2.06×10^{2}	1.76×10^{2}
	N3	11.92	3	4.93×10^{3}	3.97×10^{5}	8.22×10^{2}	2.39×10^{2}
River	N2	14.44	8	8.46×10^{3}	4.61×10^{5}	1.41×10^{3}	2.97×10^{2}
mouth	N2	14.41	3	4.32×10^{3}	3.62×10^{5}	7.20×10^{2}	2.13×10^{2}
	N1	17.71	9	3.01×10^{3}	3.51×10^{5}	5.01×10^{2}	2.14×10^{2}
	N1	17.75	3	4.70×10^{3}	2.60×10^{5}	7.83×10^{2}	1.63×10^{2}
	Y0	0.20	7	1.01×10^{3}	6.77×10^{4}	1.68×10^{2}	3.93×10^{1}
	Y0	0.20	3	3.00×10^{2}	4.19×10^{4}	5.00×10^{1}	2.46×10^{1}
	Y1	23.06	8	1.47×10^{4}	5.20×10^{4}	2.45×10^{3}	2.81×10^{1}
	Y1	21.22	3	1.92×10^{4}	4.14×10^{4}	3.19×10^{3}	2.63×10^{1}
	Y2	29.31	16	2.75×10^{4}	2.19×10^{4}	4.59×10^{3}	1.20×10^{1}
	Y2	29.37	10	9.48×10^{3}	1.94×10^{4}	1.58×10^{3}	1.01×10^{1}
	Y2	29.00	3	4.91×10^{3}	1.35×10^{4}	8.38×10^{2}	6.03×10^{0}
	Y3	30.25	21	3.47×10^{3}	2.88×10^{4}	8.19×10^{2}	1.60×10^{1}
	Y3	29.59	10	3.26×10^{3}	1.03×10^{4}	5.79×10^{2}	5.19×10^{0}
Inner	Y3	27.46	3	5.03×10^{3}	6.17×10^{4}	5.43×10^{2}	3.10×10^{0}
plume	2Y3	30.55	20	5.84×10^{3}	1.23×10^{4}	9.73×10^{2}	6.10×10^{0}
	2Y3	30.07	10	2.45×10^{3}	7.30×10^{3}	4.08×10^{2}	2.85×10^{0}
	2Y3	27.88	3	1.70×10^{3}	1.64×10^{3}	2.84×10^{2}	3.93×10^{-1}
	3Y3	32.19	20	5.03×10^{3}	8.25×10^{3}	8.38×10^{2}	5.48×10^{0}
	3Y3	30.10	10	2.53×10^{3}	4.53×10^{3}	4.22×10^{2}	1.23×10^{0}
	3Y3	27.92	3	6.89×10^{2}	2.10×10^{3}	1.15×10^{2}	5.56×10^{-1}
	N0	26.79	21	8.81×10^{3}	2.27×10^{4}	1.47×10^{3}	1.64×10^{1}
	N0	26.52	10	1.60×10^{3}	8.45×10^{3}	2.67×10^{2}	4.92×10^{0}
	N0	25.83	3	1.71×10^{3}	9.78×10^{3}	2.85×10^{2}	5.85×10^{0}
	Y4	34.39	50	2.73×10^{3}	3.60×10^{3}	4.55×10^{2}	1.63×10^{0}
	Y4	34.36	30	3.26×10^{3}	2.49×10^{3}	5.43×10^{2}	1.32×10^{0}
	Y4	33.42	20	6.75×10^{2}	7.97×10^{1}	1.13×10^{2}	5.10×10^{-2}
	Y4	30.67	10	9.16×10^{1}	7.42×10^{1}	1.53×10^{1}	1.09×10^{-2}
Outer	Y4	28.33	3	BDL	1.70×10^{2}	BDL	2.83×10^{-2}
plume	Y5	34.30	46	1.01×10^{2}	1.66×10^{3}	1.68×10^{1}	8.36×10^{-1}
	Y5	34.30	30	1.97×10^{2}	1.31×10^{3}	3.28×10^{1}	1.03×10^{0}
	Y5	33.96	20	BDL	7.70×10^{1}	BDL	4.66×10^{-2}
	Y5	32.52	10	1.48×10^{1}	1.13×10^{2}	2.47×10^{0}	6.42×10^{-2}
	Y5	30.41	3	BDL	4.88×10^{2}	BDL	4.44×10^{-2}

[a] The calculation of Fe(III) demand was based on Eq. (3) by assuming six mole of Fe(III) was needed to oxidize one mole ammonium to nitrite.
[b] The calculation of Mn(IV) demand was based on Eq. (4) by assuming one mole of Mn(IV) was needed to oxidize one mole of nitrite to nitrate.
BDL means below detection limit.

BGD
10, 8685–8713, 2013

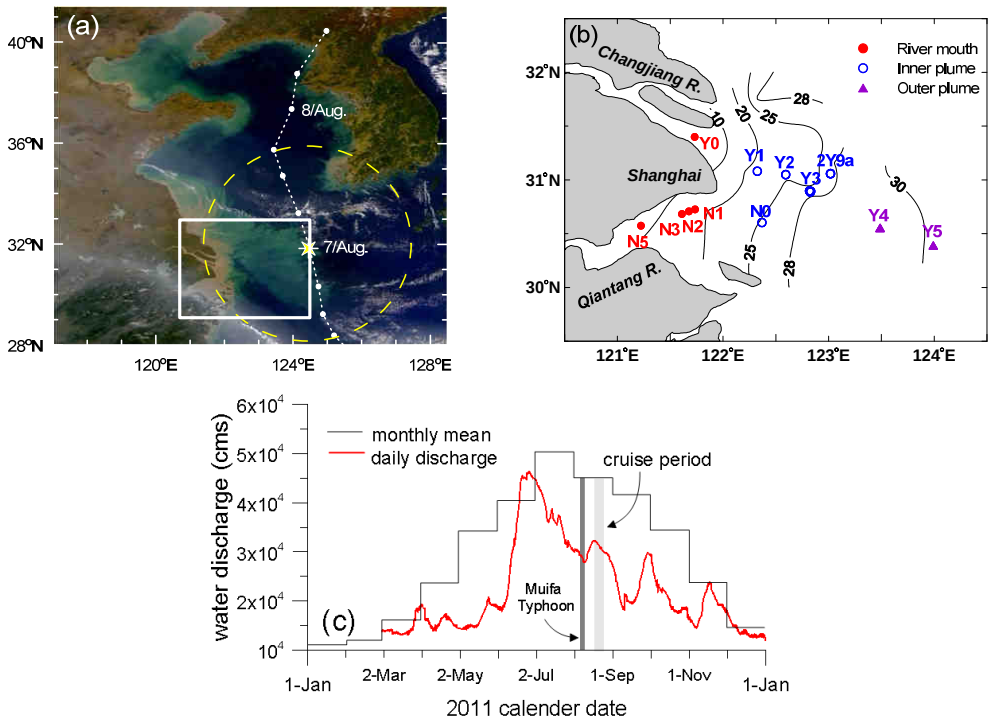

Fig. 1. (a) The satellite image of the Yellow sea, Bohai Sea and the East China Sea. Note that turbid water features the coastal zone and the river mouths. White rectangle represents our study site. The white dashed line is trajectory of Muifa, and the yellow dashed circle indicates cloud coverage of Muifa (average wind speed > 14 $m s^{-1}$) at 0.00 a.m., 7 August. **(b)** The map of sampling stations. Contours stand for the sea surface salinity. The sampling stations were classified as river mouth (•), inner plume (◦) and outer plume (▲). Station names were marked. **(c)** The long-term monthly mean water discharge (solid black) and daily discharge (red curve) at Datong, the most downstream gauge, of the Changjiang River. Dark gray bar represents the period influenced by Typhoon Muifa and light gray stands for the cruise period.

BGD
10, 8685–8713, 2013

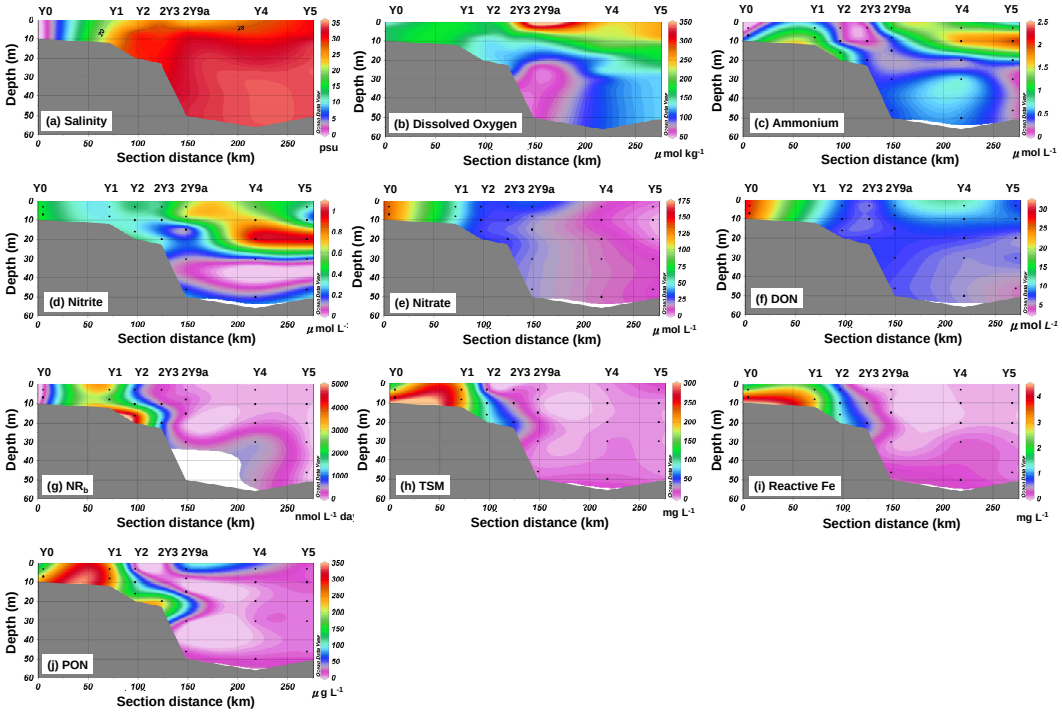

Fig. 2. Transects of **(a)** Salinity, **(b)** dissolved oxygen, **(c)** ammonium, **(d)** nitrite, **(e)** nitrate, **(f)** dissolved organic nitrogen (DON), **(g)** bulk nitrification rate (NR_b), **(h)** total suspended material, **(i)** reactive Fe, **(j)** particulate organic nitrogen (PON) across the Changjiang plume. Salinity and dissolved oxygen were obtained continuously by CTD. Discrete sampling depths of other parameters are indicated by black dot. Data were plotted using the DIVA gridding in ocean data view v.4.3.2 (http://odv.awi.de, 2010).

BGD
10, 8685–8713, 2013

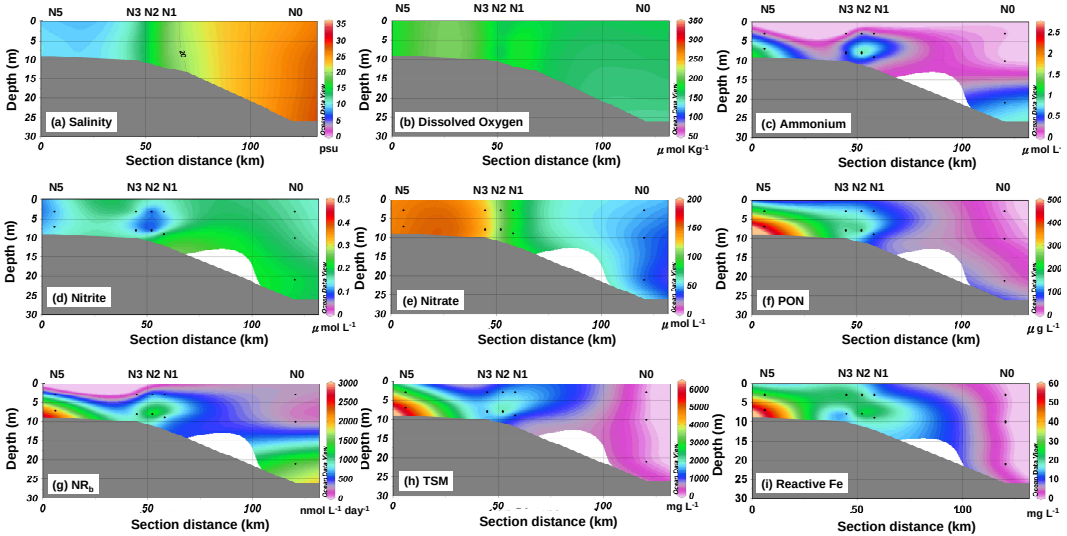

Fig. 3. Transects of **(a)** Salinity, **(b)** dissolved oxygen, **(c)** ammonium, **(d)** nitrite, **(e)** nitrate, **(f)** particulate organic nitrogen (PON), **(g)** bulk nitrification rate (NR_b), **(h)** total suspended material, **(i)** reactive Fe, across the Qiantang River mouth. The color mapping represents the same range of data in Fig. 2 except for PON, TSM and reactive Fe. Salinity and dissolved oxygen were obtained continuously by CTD. Discrete sampling depths of other parameters are indicated by black dot. Data were plotted using the DIVA gridding in ocean data view v.4.3.2 (http://odv.awi.de, 2010).

BGD
10, 8685–8713, 2013

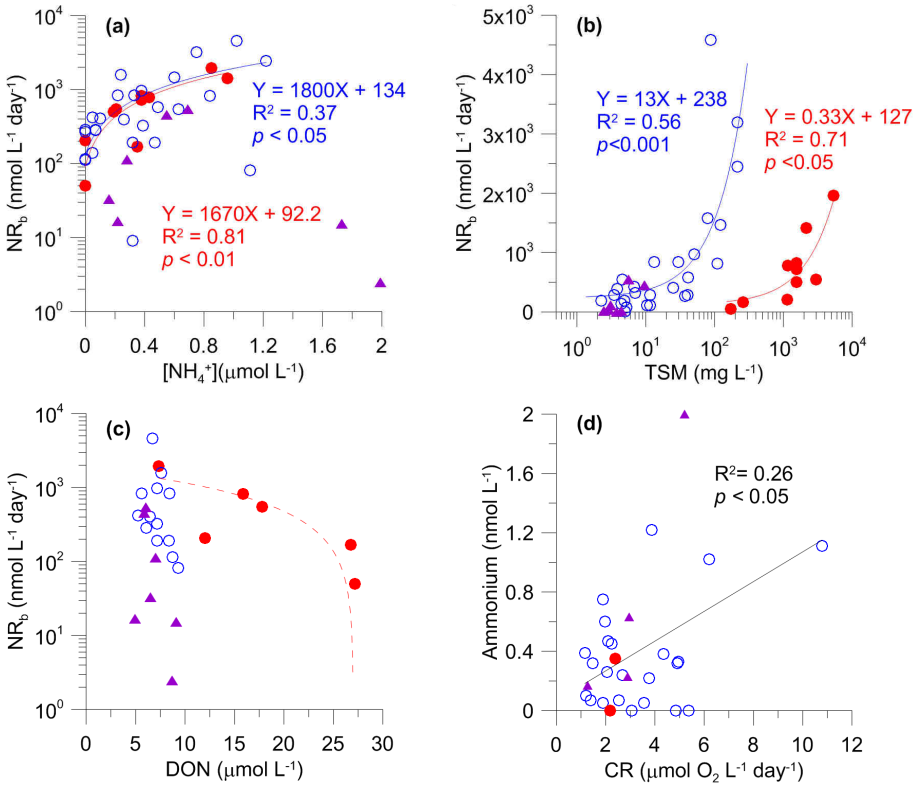

Fig. 4. Scatter plot of bulk nitrification rate against **(a)** ammonium, **(b)** TSM and **(c)** DON along the Changjiang River plume and the Qiantang River mouth. The symbols indicate the data from river mouth (•), inner plume (◦), or outer plume (▲). The blue and red curves indicate the linear regression in log-log scale for inner plume and river mouth, respectively. **(d)** Scatter plot of CR vs. ammonium. Linear regression line for all data points was shown.

BGD
10, 8685–8713, 2013

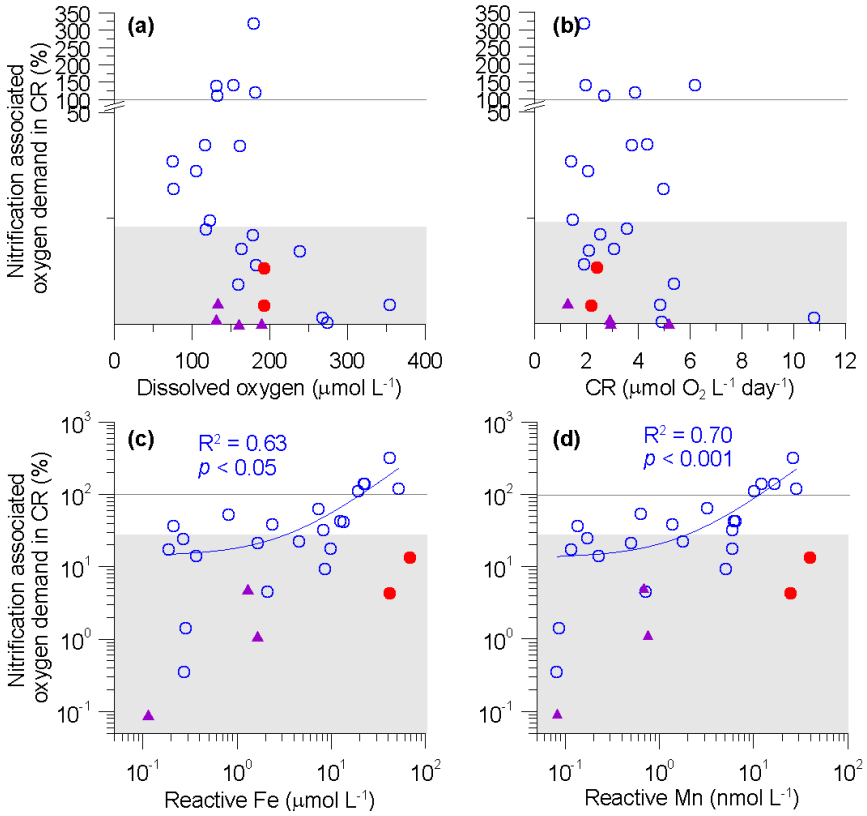

Fig. 5. The scatter plots of the percentage of nitrification-associated oxygen demand in CR against **(a)** dissolved oxygen, **(b)** community respiration rate, **(c)** reactive Fe and **(d)** reactive Mn for river mouth (•), inner plume (∘) and outer plume (▲). Data for Qiantang River mouth and Y4 station were not included because of lacking of community respiration rate data. The shaded zone with upper limit of 23.2 % indicates the theoretical estimate by Redfield model. The horizontal line referred to 100 % CR.

BGD
10, 8685–8713, 2013